

A Tractable Analytical Framework for Evaluating Opportunistic Selection in Time-Varying Channels

Rupesh K. Kona, *Student Member, IEEE*, Neelesh B. Mehta, *Senior Member, IEEE*, and Jobin Francis

Abstract—Time-variations in wireless channels affect opportunistic selection in a multi-node wireless system in two ways. First, the selected node can become sub-optimal by the time data transmission commences. Second, the channel changes during data transmission. We develop a comprehensive and tractable analytical framework that accurately accounts for both these effects. It differs from the extensive existing literature that primarily focuses on time-variations until the data transmission starts. We first develop a novel concept of a time-invariant effective signal-to-noise ratio (TIESNR), which tractably and accurately captures the time-variations during the data transmission phase with partial channel state information available at the receiver. Thereafter, we model the joint distribution of the signal-to-noise ratio at the time of selection and TIESNR during the data transmission and analyze the average packet error rate (PER). Extensive numerical results verify the accuracy of each step of our approach and show that ignoring the correlated time-variations during the data transmission phase can significantly underestimate the average PER.

I. INTRODUCTION

Current multi-node wireless systems such as cellular systems, wireless local area networks (WLANs), and cooperative systems employ opportunistic selection to improve the spectral and energy efficiency. Cellular systems and WLANs exploit multi-user diversity by making the base station or access point opportunistically select and transmit to the user with the highest instantaneous signal-to-noise ratio (SNR) [1]. Similarly, cooperative systems exploit spatial diversity by opportunistically selecting one among the available relays [2].

Opportunistic selection, while appealing, is difficult to implement because the wireless nodes are geographically separated and no node in the system knows all the channel gains a priori. Hence, selection schemes such as polling [3], timer [2], [4], or splitting [3] are required to select the best node. During the time duration required to select the best node, the channel state changes, as a result of which a node that is sub-optimal for the channel conditions at the time of data transmission may be chosen. The channel also changes during the data transmission duration. These together degrade the system throughput.

A. Related Literature

Given its practical importance, the effect of outdated channel state information (CSI) on opportunistic selection has been extensively investigated in the literature on cellular and cooperative systems. In [5], [6] and the references therein,

the effect of feedback delay on the average throughput of a cellular system with different schedulers is analyzed. In [7], its effect on the average throughput of a greedy scheduler for an adaptive, multi-user orthogonal frequency-division multiplexing (OFDM) system with uncoded M-QAM is analyzed.

In [8], the impact of outdated CSI on the outage probability and the average bit error rate when the k^{th} worst amplify-and-forward relay is selected is analyzed. In [9], its effect on the outage probability for decode-and-forward relaying is analyzed. While [8], [9] and other references such as [10], [11] focus on uncoded packets, relay selection for coded cooperative networks with outdated CSI is analyzed in [12].

In all the above papers, the channel is assumed to remain constant over the entire duration of data transmission. Only its variations during the selection phase are tracked to ensure analytical tractability. This is practically unrealistic when the data transmission duration is comparable to or greater than the selection duration. This is typically the case in order to reduce the spectral efficiency loss due to the time spent on selection. While time variations during data transmission were modeled in [13], only Monte Carlo simulation results were presented and the receiver was assumed to know the channel gain seen by every symbol in a packet.

B. Contributions

In this paper, we develop a novel analytical framework to accurately characterize the combined effect of time variations during the selection and data transmission phases on the packet error rate (PER). Our approach has the following advantages: (i) It accounts for the channel variation during the data transmission phase. (ii) It accounts for the fact that a receiver, which estimates the channel from a few pilot symbols, has only partial CSI because it cannot know perfectly the channel gains seen by all the symbols in the packet in a time-varying channel. (iii) It captures the correlation between the channel gains at the time of selection and during data transmission, which is necessary for selection to be effective. (iv) It models the use of the same modulation and coding scheme (MCS) for all symbols in a packet.

We first propose and verify a novel time-invariant effective SNR (TIESNR) approach for modeling the impact of time variations during the data transmission phase with partial CSI available at the receiver. It maps the vector of SNRs into a single SNR, which can be interpreted as the equivalent SNR of the packet transmitted over an additive white Gaussian noise (AWGN) channel. This approach enables the well understood results on PER in AWGN channels to be applied to our problem, and works for any MCS.

The authors are with the Dept. of Electrical Communication Eng. at the Indian Institute of Science (IISc), Bangalore, India.

Emails: rupeshkumarkona@gmail.com, nbmehta@ece.iisc.ernet.in, and jobin@ece.iisc.ernet.in.

Next, we model the significant correlation between the SNR at the time of selection and TIESNR during data transmission. For this, we model their joint distribution as the generalized bivariate gamma distribution (GBGD), which is provably exact as the correlation coefficient approaches unity. Another advantage is that the GBGD parameters are easily determined by matching its moment generating function (MGF) at three carefully chosen points with that of TIESNR, for which we derive closed-form expressions. The above steps culminate in a novel expression for the average PER. We present extensive numerical results to verify the accuracy of our entire approach. We observe that the time-invariant model considered in the literature significantly underestimates the average PER of many MCSs even for packet durations as small as 1 msec.

C. Organization and Notations

Section II describes the system model. Section III develops the TIESNR approach. Average PER is analyzed in Section IV. Numerical results and our conclusions follow in Sections V and VI, respectively.

Notations: $\Pr(\cdot)$ denotes probability. For a complex number c , $|c|$, c^* , and $\text{Re}\{c\}$ denote its absolute value, complex conjugate, and real part, respectively. For a random variable (RV) X , $\mathbb{E}[X]$ and $f_X(x)$ denote expectation and probability density function (PDF), respectively. For two RVs X and Y , the conditional PDF of Y given $X = x$ is denoted by $f_Y(y|X = x)$. The joint MGF $\Psi_{X,Y}(s_1, s_2)$ of RVs X and Y evaluated at (s_1, s_2) is defined as $\mathbb{E}[\exp(-s_1X - s_2Y)]$.

II. SYSTEM MODEL

We consider a system that consists of a source S and M users. The channel gains of the source-user links are assumed to be independent and identically distributed (i.i.d.) [5], [7]–[10]. The baseband channel gain from S to user k at time $t = iT_s$ is denoted by $h_i^{(k)}$, where T_s is the symbol duration. It is a complex Gaussian random process and evolves as per the Jakes' model. Hence, $\mathbb{E}[h_i^{(k)} h_j^{(k)*}] = J_0(2\pi f_d(i-j)T_s)$, where $J_0(\cdot)$ is the zeroth order Bessel function of the first kind and f_d is the Doppler frequency. Let $\zeta_i^{(k)} = |h_i^{(k)}|^2 P_s / \sigma^2$ denote the SNR of the link from S to user k at time $t = iT_s$, where P_s and σ^2 denote the transmit power and noise variance, respectively.

The communication from S to the users occurs as follows:

1) *Selection Phase:* This phase lasts for a duration of $T_{\text{sel}} = \Delta T_s$. In it, the source first transmits a pilot at $t = 0$ for a duration of T_s . This enables all the users to estimate their respective channel gains. The user b , which is selected during this phase, is the one with the highest SNR at $t = 0$ [7]:

$$b = \arg \max_{k=1,2,\dots,M} \zeta_0^{(k)}. \quad (1)$$

In order to focus on the impact of time-varying channels, we assume that the estimates are not noisy [8], [9], though they are still partially outdated when data transmission commences.

2) *Data Transmission Phase:* The source then transmits a packet, which is generated using a pre-specified MCS of rate

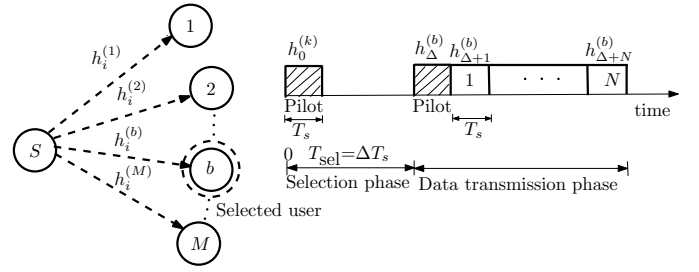


Fig. 1. System model showing a source S that selects a user among the M users and then transmits data to it.

R , to user b . To enable coherent demodulation, a pilot is embedded in the first symbol of the packet, through which the selected user b can estimate $h_{\Delta}^{(b)}$ [14]. The i^{th} received symbol $y_i^{(b)}$ at user b is given by

$$y_i^{(b)} = \sqrt{P_s} x_i h_{\Delta+i}^{(b)} + n_i, \quad \text{for } 1 \leq i \leq N, \quad (2)$$

where x_i is the i^{th} transmitted data symbol in a packet and n_i is additive white circularly symmetric complex Gaussian noise with variance σ^2 .

III. TIME-VARIATIONS DURING DATA TRANSMISSION

We now analytically characterize the effect of channel variations during the data transmission phase. For this, we first consider the simple cases of uncoded BPSK and QPSK. We then generalize the insights obtained to an arbitrary MCS.

A. TIESNR Expressions for Uncoded BPSK and QPSK

The observables at the receiver of a user k are the channel gain when selection commences $h_0^{(k)}$ and at the first symbol of the packet $h_{\Delta}^{(k)}$. Using the union bound, the PER conditioned on $h_0^{(k)}$ and $h_{\Delta}^{(k)}$, denoted by $\text{PER}(h_0^{(k)}, h_{\Delta}^{(k)})$, is bounded as

$$\text{PER}(h_0^{(k)}, h_{\Delta}^{(k)}) \leq \sum_{i=1}^N \Pr(\text{SE}_i^{(k)} | h_0^{(k)}, h_{\Delta}^{(k)}), \quad (3)$$

where $\text{SE}_i^{(k)}$ denotes the event that the i^{th} symbol is in error for the k^{th} user. Let $\mu_i = \frac{(\rho_{i0} - \rho_{i\Delta} \rho_{\Delta 0}) h_0^{(k)} + (\rho_{i\Delta} - \rho_{i0} \rho_{\Delta 0}) h_{\Delta}^{(k)}}{1 - \rho_{\Delta 0}^2}$ and $\sigma_i^2 = 1 - \frac{\rho_{i0}^2 + \rho_{i\Delta}^2 - 2\rho_{i\Delta} \rho_{i0} \rho_{\Delta 0}}{1 - \rho_{\Delta 0}^2}$ denote the mean and variance of $h_{\Delta+i}^{(k)}$ given $h_0^{(k)}$ and $h_{\Delta}^{(k)}$, respectively. Here, $\rho_{i\Delta} = \mathbb{E}[h_{\Delta+i}^{(k)} h_{\Delta}^{(k)*}] = J_0(2\pi f_d i T_s)$, $\rho_{i0} = \mathbb{E}[h_{\Delta+i}^{(k)} h_0^{(k)*}] = J_0(2\pi f_d (\Delta + i) T_s)$. Similarly, $\rho_{\Delta 0} = J_0(2\pi f_d \Delta T_s)$.

For uncoded BPSK, it can be shown that $y_i^{(k)} \mu_i^*$ is a sufficient statistic to decode the i^{th} symbol. Therefore, from (3),

$$\begin{aligned} \text{PER}(h_0^{(k)}, h_{\Delta}^{(k)}) & \leq \sum_{i=1}^N \Pr(\text{Re}\{y_i^{(k)} \mu_i^*\} < 0 | h_0^{(k)}, h_{\Delta}^{(k)}, x_i = 1). \end{aligned} \quad (4)$$

From (2), it is also clear that $\text{Re}\{y_i^{(k)} \mu_i^*\}$ conditioned on $h_0^{(k)}, h_{\Delta}^{(k)}$, and $x_i = 1$ is a Gaussian RV with mean $\sqrt{P_s} |\mu_i|^2$

and variance $|\mu_i|^2 (P_s \sigma_i^2 + \sigma^2) / 2$. Using the Chernoff bound,

$$\text{PER} \left(h_0^{(k)}, h_\Delta^{(k)} \right) \leq \frac{1}{2} \sum_{i=1}^N \exp \left(\frac{-P_s |\mu_i|^2}{P_s \sigma_i^2 + \sigma^2} \right). \quad (5)$$

If the channel were time-invariant with its SNR being $\gamma_{\text{eff}}^{(k)}$ over the packet duration, then the upper bound in (5) reduces to $\frac{N}{2} \exp(-\gamma_{\text{eff}}^{(k)})$. Equating the two, we get

$$\gamma_{\text{eff}}^{(k)} = -\log \left(\frac{1}{N} \sum_{i=1}^N \exp \left(\frac{-P_s |\mu_i|^2}{P_s \sigma_i^2 + \sigma^2} \right) \right). \quad (6)$$

For uncoded QPSK, a similar derivation yields

$$\gamma_{\text{eff}}^{(k)} = -2 \log \left(\frac{1}{N} \sum_{i=1}^N \exp \left(\frac{-\frac{P_s}{2} |\mu_i|^2}{\frac{P_s}{2} \sigma_i^2 + \sigma^2} \right) \right). \quad (7)$$

B. TIESNR Expression for Any MCS

We notice that only an additional factor of 2 appears at three places in (7) compared to (6). This motivates generalizing the above expression to any arbitrary MCS as follows:

$$\gamma_{\text{eff}}^{(k)} = -\beta \log \left(\frac{1}{N} \sum_{i=1}^N \exp(-a_i |\mu_i|^2) \right), \quad (8)$$

where $a_i = \frac{P_s \beta^{-1}}{P_s \sigma_i^2 \beta^{-1} + \sigma^2}$. The term β is an MCS-dependent scaling parameter that is tuned numerically. Note that this needs to be done only once for any given MCS and speed. The calibration of β and the accuracy of this generalization for over three orders of magnitude of PER for different MCSs and speeds shall be investigated in Section V-A.

Comments: We note that, in general, the symbol error probability (SEP) of many MCSs is well approximated by the formula $c_1 \exp(-c_2 \gamma)$, where γ is the SNR at the time of symbol transmission (assuming perfect CSI at receiver) and c_1 and c_2 are MCS-dependent parameters [15, Chap. 9.4]. Thus, even when perfect CSI is available for all symbols, the SNR is scaled by a modulation-dependent parameter c_2 . This intuition carries over to the coded packet as well when one considers the widely used code-dependent coding loss approach [16]. Even here, the SNR is scaled by a factor that depends on the practical code used.

The TIESNR derivation above is motivated by the success of link quality metrics such as exponential effective SNR mapping (EESM), which have been widely used for modeling the channel variations in the frequency-domain in OFDM systems [17], [18]. However, in [17], [18], the channel gains across all the symbols are assumed to be known at the receiver. On the other hand, in our model, the receiver has only partial CSI. Unlike EESM, the SNRs of different symbols in TIESNR are scaled by different factors a_1, \dots, a_N . The conditional means μ_1, \dots, μ_N are also different for different symbols. This captures the impact of increasingly outdated CSI, while decoding later symbols in a packet. Unlike EESM, which is a function of N subcarrier channel gains, TIESNR is only a function $h_0^{(k)}$ and $h_\Delta^{(k)}$. Consequently, TIESNR depends on not just the MCS, but also the speed, which is unlike EESM.

IV. AVERAGE PER ANALYSIS

The average PER, denoted by $\overline{\text{PER}}$, is given by

$$\overline{\text{PER}} = \mathbb{E} \left[\text{PER} \left(h_0^{(b)}, h_\Delta^{(b)} \right) \right]. \quad (9)$$

From the TIESNR concept, the average PER expression becomes

$$\overline{\text{PER}} = \mathbb{E} \left[\text{PER} \left(\gamma_{\text{eff}}^{(b)} \right) \right], \quad (10)$$

where the notation $\text{PER} \left(\gamma_{\text{eff}}^{(b)} \right)$ captures the fact that the PER depends only on $\gamma_{\text{eff}}^{(b)}$. From the law of total expectation,

$$\overline{\text{PER}} = \int_0^\infty \int_0^\infty \text{PER}(z) f_{\gamma_{\text{eff}}^{(b)}}(z | \zeta_0^{(b)} = y) f_{\zeta_0^{(b)}}(y) dz dy. \quad (11)$$

We now evaluate each term in the integrand above. First, from Bayes' rule and since the channel gains of different users are i.i.d., we get $f_{\gamma_{\text{eff}}^{(b)}}(z | \zeta_0^{(b)} = y) = \frac{f_{\zeta_0^{(1)}, \gamma_{\text{eff}}^{(1)}}(y, z)}{f_{\zeta_0^{(1)}}(y)}$. Second, from order statistics, we know that $f_{\zeta_0^{(b)}}(y) = \frac{M \sigma^2}{P_s} \left(1 - e^{-\frac{y \sigma^2}{P_s}} \right)^{M-1} e^{-\frac{y \sigma^2}{P_s}}$, for $y \geq 0$. Third, for AWGN channels, the PER is well approximated by an exponential function of the effective SNR as follows [19]:

$$\text{PER} \left(\gamma_{\text{eff}}^{(b)} \right) = \begin{cases} 1, & 0 < \gamma_{\text{eff}}^{(b)} < \gamma_p, \\ \alpha \exp(-\delta \gamma_{\text{eff}}^{(b)}), & \gamma_{\text{eff}}^{(b)} \geq \gamma_p, \end{cases} \quad (12)$$

where α and δ are MCS-dependent parameters, and $\gamma_p = (\log(\alpha))/\delta$. The process for determining α and δ and its accuracy are discussed in Section V-A. While such an approximation has been used in [19], the channel was assumed to remain constant and known perfectly during the packet duration.

The last step is to find the joint PDF $f_{\zeta_0^{(1)}, \gamma_{\text{eff}}^{(1)}}(y, z)$. It is not available in closed-form because of the non-linear nature of $\gamma_{\text{eff}}^{(1)}$. To gain intuition, consider the low speed regime in which $\rho_{i\Delta} \approx \rho_{i0} \approx \rho_{\Delta 0} \approx 1$, for all i . It can then be shown that $\zeta_0^{(1)}$ and $\gamma_{\text{eff}}^{(1)}$ follow the joint exponential distribution, which is a special case of GBGD. We, therefore, propose modeling the joint distribution of $\zeta_0^{(1)}$ and $\gamma_{\text{eff}}^{(1)}$ as GBGD. As we shall see in Section V-B, GBGD possesses sufficient parametric flexibility to be accurate even for higher speeds.

The GBGD of two RVs Y_1 and Y_2 is specified in terms of five parameters $p_1, p_2, q_1, q_2 > 0$, and $0 \leq \mu < 1$ as [20]:

$$f_{Y_1, Y_2}(y_1, y_2) = (1 - \mu)^{q_2} e^{-m y_1 - a y_2} \left[\sum_{h=0}^{\infty} \frac{(q_1)_h \mu^h}{\Gamma(q_1 + h) h!} \times {}_1F_1(q_2 - q_1; q_2 + h; \mu y_2 a) \frac{(m y_1)^{q_1 + h} (a y_2)^{q_2 + h}}{y_1 y_2 \Gamma(q_2 + h)} \right], \quad (13)$$

for $y_1 \geq 0$ and $y_2 \geq 0$, where $m = \frac{1}{p_1(1-\mu)}$, $a = \frac{1}{p_2(1-\mu)}$, μ is the correlation coefficient between Y_1 and Y_2 , ${}_1F_1(a, b; z)$ is the confluent hypergeometric function [21, (9.210.1)], $\Gamma(\cdot)$ is the gamma function [21, (8.310.1)], and $(a)_k$ is the Pochhammer symbol [21, pp. xliii].

A. Determining Parameters of GBGD Model

Now, we evaluate the parameters of GBGD. Since $\zeta_0^{(1)}$ is an exponentially distributed RV, we have $p_1 = P_s/\sigma^2$ and $q_1 = 1$. The parameters p_2 , q_2 , and μ are evaluated by matching the joint MGF of $\zeta_0^{(1)}$ and $\gamma_{\text{eff}}^{(1)}$ with that of the GBGD at three carefully chosen points at which the MGF takes a simple closed-form, as shown below.

Result 1: The joint MGF of $\zeta_0^{(1)}$ and $\gamma_{\text{eff}}^{(1)}$ evaluated at points $(0, 2\beta^{-1})$ and (z, β^{-1}) , where $z \geq 0$, are given by

$$\Psi_{\zeta_0^{(1)}, \gamma_{\text{eff}}^{(1)}}(0, 2\beta^{-1}) = \frac{1}{N^2} \times \sum_{i=1}^N \sum_{j=1}^N \left(1 + a_i \sigma_{\mu_i}^2 + a_j \sigma_{\mu_j}^2 + a_i a_j (1 - \phi_{ij}) \sigma_{\mu_i}^2 \sigma_{\mu_j}^2\right)^{-1}, \quad (14)$$

$$\Psi_{\zeta_0^{(1)}, \gamma_{\text{eff}}^{(1)}}(z, \beta^{-1}) = \frac{1}{N} \times \sum_{i=1}^N \left(1 + a_i \sigma_{\mu_i}^2 + \frac{P_s}{\sigma^2} z + z a_i (1 - \eta_i) \sigma_{\mu_i}^2 \frac{P_s}{\sigma^2}\right)^{-1}, \quad (15)$$

where $\sigma_{\mu_i}^2 = K_{i1}^2 + K_{i0}^2 + 2K_{i1}K_{i0}\rho_{\Delta 0}$, $\eta_i = (K_{i0}^2 + K_{i1}^2 \rho_{\Delta 0}^2 + 2K_{i1}K_{i0}\rho_{\Delta 0}) \sigma_{\mu_i}^{-2}$, $\phi_{ij} = (K_{i1}K_{j1} + K_{i0}K_{j0} + K_{i1}K_{j0}\rho_{\Delta 0} + K_{i0}K_{j1}\rho_{\Delta 0})^2 \sigma_{\mu_i}^{-2} \sigma_{\mu_j}^{-2}$, $K_{i1} = \frac{\rho_{i0} \rho_{i\Delta 0}}{1 - \rho_{\Delta 0}^2}$, and $K_{i0} = \frac{\rho_{i0} - \rho_{i\Delta 0} \rho_{\Delta 0}}{1 - \rho_{\Delta 0}^2}$.

Proof: The proof is relegated to Appendix A. ■

The joint MGF of two RVs Y_1 and Y_2 that follow GBGD, evaluated at $s_1 \geq 0$ and $s_2 \geq 0$, is given by [20]

$$\Psi_{Y_1, Y_2}(s_1, s_2) = \frac{(s_2 p_2 + 1)^{q_1 - q_2}}{(s_1 s_2 p_1 p_2 (1 - \mu) + s_1 p_1 + s_2 p_2 + 1)^{q_1}}. \quad (16)$$

The MGF expressions in (14), (15), and (16) are matched at the points $(0, \beta^{-1})$, $(0, 2\beta^{-1})$, and (z, β^{-1}) . The first two points help solve for p_2 and q_2 . The third point helps solve for μ . The value of μ turns out to be insensitive to choice of z , which is, therefore, set to 10 henceforth.

B. Average PER Expression

Given the joint PDF of $f_{\zeta_0^{(1)}, \gamma_{\text{eff}}^{(1)}}(y, z)$, the average PER can be derived in closed-form as shown below.

Result 2: The average PER is given as

$$\overline{\text{PER}} = M (1 - \mu)^{q_2} \sum_{i=0}^{M-1} \sum_{k=0}^{\infty} \sum_{n=0}^{\infty} \frac{(m p_1)^{k+1} \mu^{n+k} (q_2 - 1)_n}{\Gamma(q_2 + k) n! (q_2 + k)_n} \times \frac{(-1)^{M-1+i} \binom{M-1}{i}}{(M-1 + p_1 m - i)^{k+1}} \left[\alpha \left(\frac{a}{a + \delta} \right)^{q_2 + k + n} (\Gamma(q_2 + n + k) - \Gamma_{\text{inc}}(q_2 + k + n, a \gamma_p + \delta \gamma_p)) + \Gamma_{\text{inc}}(q_2 + k + n, a \gamma_p) \right], \quad (17)$$

where $\Gamma_{\text{inc}}(x, s)$ is the incomplete gamma function [21, (8.350.1)].

Proof: The proof is relegated to Appendix B. ■

The above result brings out the dependence of $\overline{\text{PER}}$ on the number of users M and the parameters of the GBGD, which,

TABLE I
VALUES OF β FOR DIFFERENT MCSs USED IN WiMAX

Rate (R)	4-QAM		16-QAM		64-QAM	
	0.5	0.75	0.5	0.75	0.5	0.75
$v = 30$ kmph	1.25	4.66	2.43	6.95	6.23	20.51
$v = 60$ kmph	1.53	1.56	2.63	5.65	9.05	8.65

in turn, depend on system parameters such as speed v and delay T_{sel} . In practice, 30 to 40 terms in the infinite series in (17) are sufficient to ensure numerical accuracy.

V. NUMERICAL RESULTS AND COMPARISONS

In summary, our approach consists of three steps. First, we capture the time-variations during the data transmission phase using TIESNR, which uses an MCS-dependent parameter β . This is inspired by the success of the EESM approach, which is widely used for characterizing the PER in OFDM [17]. Second, in (12), we approximate the PER to be an exponentially decaying function of a single parameter, which is the effective SNR. This circumvents the problem that no closed-form expression for the PER of an arbitrary MCS is available for partial CSI and time-varying channels. Finally, we used GBGD to model the joint distribution of the SNR at the time of selection and the effective SNR during data transmission. We now verify the accuracy of each of these steps and our entire approach for different system parameters.

A. Calibration of β for MCSs and Verification of TIESNR

We first illustrate how β is calibrated for any given MCS. We do so for duo-binary tail-biting convolutional turbo codes (CTC) of block length $N = 48$, which are employed in WiMAX [22]. For this, we consider $n = 10^5$ traces of the channel gains seen over the packet duration. These are generated using the Jakes' model. For the i^{th} channel trace, the probability P_i that the packet is in error conditioned on $h_0^{(k)}$ and $h_{\Delta}^{(k)}$ is measured using bit-level simulations that implement the demodulation and turbo decoding process at the receiver and average over 10^5 noise sample traces. For the same channel trace, we compute TIESNR as a function of β using (8). Plotting the pairs $(\gamma_{\text{eff}_i}(\beta), P_i)$, for $1 \leq i \leq n$, yields a *scatter plot*.

On the same plot, we also plot the average PER for the same MCS as a function of the average SNR P_s/σ^2 for an AWGN (time-invariant) channel. We shall refer to this as the *AWGN reference curve*. Let γ_{AWGN_i} represent the AWGN SNR at which the PER is P_i . Then, β is chosen to minimize the square of the difference in dB between $(\gamma_{\text{AWGN}_1}, \dots, \gamma_{\text{AWGN}_n})$ and $(\gamma_{\text{eff}_1}(\beta), \dots, \gamma_{\text{eff}_n}(\beta))$ [17]. The difference is taken in dB scale in order to ensure that PERs as low as 0.001 are given importance. The calibrated β values are shown in Table I for different MCSs and for different speeds.

Figure 2 plots the scatter plot for the calibrated β and the AWGN reference curves for 4, 16 and 64 QAM with $R = 0.5$. Since the users are i.i.d., by default we show our results for user 1. The minimal spread in the y-direction of the scatter plot and its closeness to the AWGN reference curve show

TABLE II
CURVE-FIT PARAMETERS OF PER IN AN AWGN CHANNEL

Rate (R)	4-QAM		16-QAM		64-QAM	
	0.5	0.75	0.5	0.75	0.5	0.75
α	143.20	220.31	114.67	622.96	247.93	427.36
δ	4.77	2.58	1.03	0.60	0.29	0.15

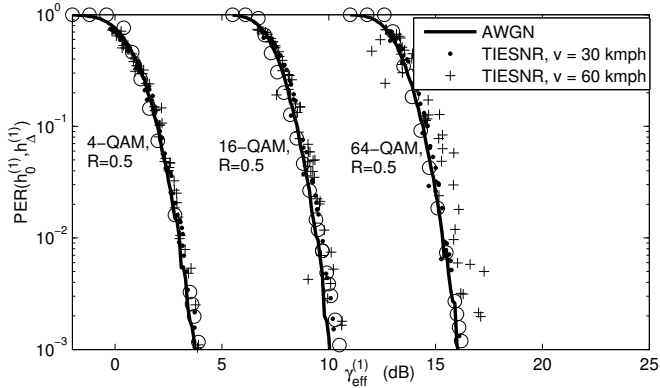


Fig. 2. Comparison of scatter plot and AWGN reference curve for different MCSs and speeds ($N = 48$, $f_c = 2$ GHz, and $T_s = 20 \mu s$). Also shown are the curve-fits for the AWGN reference curves (cf. (12)) using marker ‘o’.

that the TIESNR approach works for different MCSs. Even at higher speeds, the match between the scatter plot and the reference curve, while not perfect, is reasonably good. Also plotted is (12), which is fit to the AWGN reference curve using the least squares criterion. We see that the curve-fit is accurate. Table II lists the values of α and δ for different MCSs.

B. Verification of GBGD Model

To visualize the accuracy of the proposed model, we plot the empirical conditional cumulative distribution function (CDF), of $\gamma_{\text{eff}}^{(1)}$ given $\zeta_0^{(1)}$ for different values of $\zeta_0^{(1)}$ in Fig. 3. It is generated using 10^5 samples. We compare it with the conditional CDF obtained from the GBGD model. We do so for $v = 60$ kmph in order to test the proposed approach not just at low speeds, which motivated it, but also at higher speeds. For all $\zeta_0^{(1)}$, the proposed GBGD model tracks the empirical curves well for $\gamma_{\text{eff}}^{(1)}$ as low as 0.06.

C. Average PER Results for Different MCSs

We present bit-level simulation results that are averaged over 10^5 packets to evaluate the accuracy of the average PER analysis. Results are shown for 4-QAM, $R = 0.5$ and 16-QAM, $R = 0.5$. Unless mentioned otherwise, $N = 48$, $f_c = 2$ GHz, $T_s = 20 \mu s$, and $T_{\text{sel}} = 0.75NT_s$. This corresponds to a packet duration of 0.96 msec.

Figure 4 plots the average PER as a function of the average SNR for different speeds with $M = 3$. The good match between the analysis and simulations validates the TIESNR-based approach, the calibration of β , and the GBGD joint PDF model, which together led to (17). Also plotted is the average PER for the time-invariant models of [8]–[12], which assume that the channel remains unchanged during data transmission.

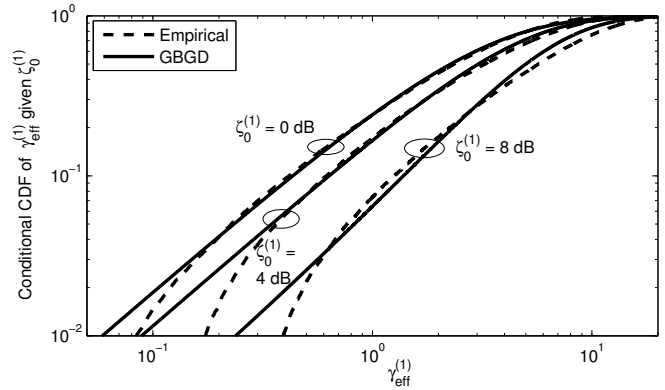


Fig. 3. $v = 60$ kmph: Conditional CDF of $\gamma_{\text{eff}}^{(1)}$ given $\zeta_0^{(1)}$ ($P_s/\sigma^2 = 10$ dB, $N = 48$, $f_c = 2$ GHz, $T_s = 20 \mu s$, $T_{\text{sel}} = 0.75NT_s$, and $\beta = 1.53$).

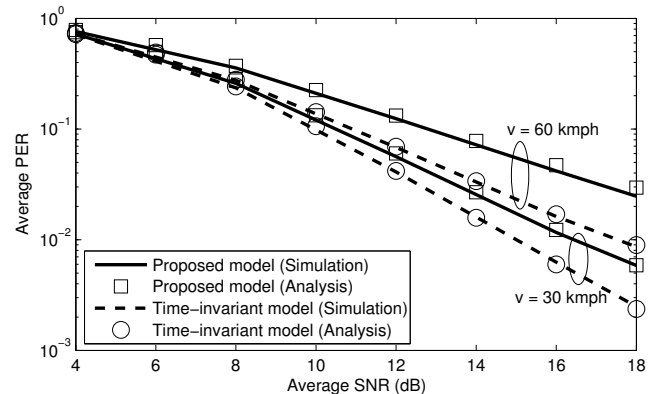


Fig. 4. Average PER as a function of average SNR for different speeds (16-QAM, $R = 0.5$, and $M = 3$).

We see that ignoring the time variations during the data transmission phase markedly underestimates the average PER. For instance, at an average SNR of 14 dB and $v = 60$ kmph, it underestimates the average PER by a factor of 2.3.

Figure 5 plots the average PER as a function of the average SNR for different numbers of users for $v = 60$ kmph. We again observe a good match between the analysis and simulations. The average PER decreases as the number of users increases, which is due to multi-user diversity. Neglecting time variations in the data transmission phase again significantly underestimates the average PER.

VI. CONCLUSIONS

We developed a general analytical framework to tractably and accurately analyze the performance of opportunistic selection in time-varying channels. To account for the time variations in the data transmission phase and its correlation with the channel state at the time of selection, we proposed the TIESNR approach and the GBGD model, and verified their accuracy empirically. This led to an accurate and tractable expression for the average PER. We observed that neglecting time variations in the data transmission phase, as is often done in the literature, significantly underestimates the average PER for many MCSs and relatively small packet durations.

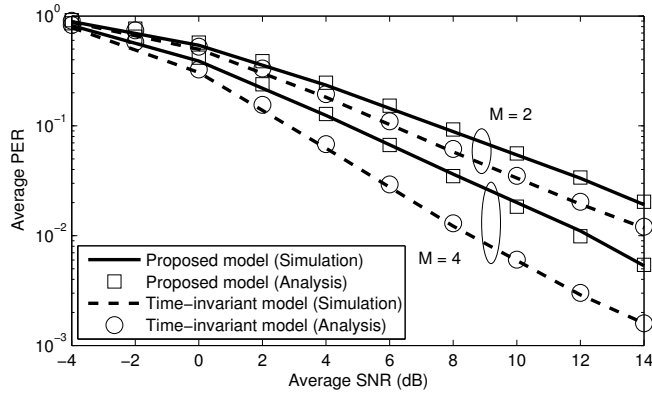


Fig. 5. Average PER as a function of average SNR for different numbers of users (4-QAM, $R = 0.5$, and $v = 60$ kmph).

APPENDIX

A. Joint MGF of $\zeta_0^{(1)}$ and $\gamma_{\text{eff}}^{(1)}$ at $(0, 2\beta^{-1})$ and (z, β^{-1})

The joint MGF of $\zeta_0^{(1)}$ and $\gamma_{\text{eff}}^{(1)}$ evaluated at $(0, 2\beta^{-1})$ is

$$\Psi_{\zeta_0^{(1)}, \gamma_{\text{eff}}^{(1)}}(0, 2\beta^{-1}) = \mathbb{E} \left[\exp \left(-2\beta^{-1} \gamma_{\text{eff}}^{(1)} \right) \right]. \quad (18)$$

Substituting the expression for $\gamma_{\text{eff}}^{(1)}$ from (8) in (18), we get

$$\Psi_{\zeta_0^{(1)}, \gamma_{\text{eff}}^{(1)}}(0, 2\beta^{-1}) = \frac{1}{N^2} \sum_{i=1}^N \sum_{j=1}^N \Psi_{|\mu_i|^2, |\mu_j|^2}(a_i, a_j). \quad (19)$$

From the μ_i expression in Section III-A, it can be shown that the joint MGF of $|\mu_i|^2$ and $|\mu_j|^2$ is given by (16) with $q_1 = 1$, $q_2 = 1$, $p_1 = \sigma_{\mu_i}^2$, $p_2 = \sigma_{\mu_j}^2$, and $\mu = \phi_{ij}$. Substituting this in (19) yields (14).

Similarly, the joint MGF of $\zeta_0^{(1)}$ and $\gamma_{\text{eff}}^{(1)}$ at (z, β^{-1}) is $\Psi_{\zeta_0^{(1)}, \gamma_{\text{eff}}^{(1)}}(z, \beta^{-1}) = \frac{1}{N} \sum_{i=1}^N \Psi_{|\mu_i|^2, \zeta_0^{(1)}}(a_i, z)$. As above, we evaluate the MGF of the bivariate exponential distribution of $|\mu_i|^2$ and $\zeta_0^{(1)}$, which is a special case of GBGD, at (a_i, z) and substitute it in the above equation to get (15).

B. Brief Derivation of Average PER Expression

From (11), the average PER is further written as

$$\overline{\text{PER}} = M \int_0^\infty \int_0^\infty \text{PER}(z) \left(1 - e^{-\frac{y\sigma^2}{P_s}} \right)^{M-1} f_{\zeta_0^{(1)}, \gamma_{\text{eff}}^{(1)}}(y, z) dy dz. \quad (20)$$

Substituting the joint PDF of $f_{\zeta_0^{(1)}, \gamma_{\text{eff}}^{(1)}}(y, z)$ from (13) and using the formula for $\text{PER}(z)$ in (12), we get

$$\begin{aligned} \overline{\text{PER}} &= M (1 - \mu)^{q_2} \sum_{k=0}^\infty \sum_{n=0}^\infty \frac{m^{k+1} \mu^{n+k} a^{q_2+k+n} (q_2 - 1)_n}{k! n! \Gamma(q_2 + k) \Gamma(q_2 + k)_n} \\ &\times \left[\int_0^\infty \left(1 - \exp \left(-\frac{y\sigma^2}{P_s} \right) \right)^{M-1} y^k \exp(-my) dy \right] \\ &\times \left[\int_0^{\gamma_p} e^{-az} z^{q_2+n+k-1} dz + \int_{\gamma_p}^\infty \alpha e^{-(a+\delta)z} z^{q_2+n+k-1} dz \right]. \end{aligned}$$

Using the identity in [21, (3.432.1)] to solve the integral over y , and writing the integral over z in terms of incomplete gamma functions, yields (17).

REFERENCES

- [1] D. Tse and P. Vishwanath, *Fundamentals of Wireless Communications*. Cambridge Univ. Press, 2005.
- [2] A. Bletsas, A. Khisti, D. P. Reed, and A. Lippman, "A simple cooperative diversity method based on network path selection," *IEEE J. Sel. Areas Commun.*, vol. 24, no. 3, pp. 659–672, Mar. 2006.
- [3] V. Shah, N. B. Mehta, and R. Yim, "Splitting algorithms for fast relay selection: Generalizations, analysis, and a unified view," *IEEE Trans. Wireless Commun.*, vol. 9, no. 4, pp. 1525–1535, Apr. 2010.
- [4] V. Shah, N. B. Mehta, and R. Yim, "Optimal timer based selection schemes," *IEEE Trans. Commun.*, vol. 58, no. 6, pp. 1814–1823, Jun. 2010.
- [5] J. L. Vicario and C. Anton-Haro, "Analytical assessment of multi-user vs. spatial diversity trade-offs with delayed channel state information," *IEEE Commun. Lett.*, vol. 10, no. 8, pp. 588–590, Aug. 2006.
- [6] S. Guharoy and N. B. Mehta, "Joint evaluation of channel feedback schemes, rate adaptation, and scheduling in OFDMA downlinks with feedback delays," *IEEE Trans. Veh. Technol.*, vol. 62, no. 4, pp. 1719–1731, May 2013.
- [7] A. Kuhne and A. Klein, "Throughput analysis of multi-user OFDMA-systems using imperfect CQI feedback and diversity techniques," *IEEE J. Sel. Areas Commun.*, vol. 26, no. 8, pp. 1440–1450, Oct. 2008.
- [8] M. Soysa, H. A. Suraweera, C. Tellambura, and H. K. Garg, "Partial and opportunistic relay selection with outdated channel estimates," *IEEE Trans. Commun.*, vol. 60, no. 3, pp. 840–850, Mar. 2012.
- [9] J. L. Vicario, A. Bel, J. A. Lopez-Salcedo, and G. Seco, "Opportunistic relay selection with outdated CSI: outage probability and diversity analysis," *IEEE Trans. Wireless Commun.*, vol. 8, no. 6, pp. 2872–2876, Jun. 2009.
- [10] M. Seyfi, S. Muhaidat, J. Liang, and M. Dianati, "Effect of feedback delay on the performance of cooperative networks with relay selection," *IEEE Trans. Wireless Commun.*, vol. 10, no. 12, pp. 4161–4171, Dec. 2011.
- [11] L. Fan, X. Lei, R. Q. Hu, and W. Seah, "Outdated relay selection in two-way relay network," *IEEE Trans. Veh. Technol.*, vol. 62, no. 8, pp. 4051–4057, Oct. 2013.
- [12] J. M. Moualeu, W. Hamouda, and F. Takawira, "Relay selection for coded cooperative networks with outdated CSI over Nakagami-m fading channels," *IEEE Trans. Wireless Commun.*, vol. 13, no. 5, pp. 2362–2373, May 2014.
- [13] S. Valentin and T. Wild, "Studying the sum capacity of mobile multiuser diversity systems with feedback errors and delay," in *Proc. VTC (Fall)*, Sep. 2010, pp. 1–5.
- [14] P. Roshan and J. Leary, *802.11 Wireless LAN Fundamentals*, 2010.
- [15] A. J. Goldsmith, *Wireless Communications*. Cambridge University Press, 2005.
- [16] T. Starr, J. M. Cioffi, and P. J. Silverman, *Understanding Digital Subscriber Line Technology*, 1st ed. Prentice Hall PTR, 1999.
- [17] E. Westman, "Calibration and evaluation of the exponential effective SINR mapping (EESM) in 802.16," Master's thesis, Royal Institute of Technology (KTH), Stockholm, Sweden, Sep. 2006.
- [18] J. Francis and N. B. Mehta, "EESM-based link adaptation in point-to-point and multi-cell OFDM systems: Modeling and analysis," *IEEE Trans. Wireless Commun.*, vol. 13, no. 1, pp. 407–417, Jan. 2014.
- [19] Q. Liu, S. Zhou, and G. B. Giannakis, "Cross-layer combining of adaptive modulation and coding with truncated ARQ over wireless links," *IEEE Trans. Wireless Commun.*, vol. 3, no. 5, pp. 1746–1755, Sep. 2004.
- [20] J. Reig, L. Rubio, and N. Cardona, "Bivariate Nakagami-m distribution with arbitrary fading parameters," *Electron. Lett.*, vol. 38, no. 25, pp. 1715–1717, Dec. 2002.
- [21] L. S. Gradshteyn and L. M. Ryzhik, *Tables of Integrals, Series and Products*. Academic Press, 2000.
- [22] R. Srinivasan, J. Zhuang, L. Jalloul, R. Novak, and J. Park, "IEEE 802.16m evaluation methodology document (EMD)," Tech. Rep. IEEE 802.16m-08/004r2, 2008.